

Load Mismatch Reduction by Energy Storage Devices as a Demand Response Program

Carlos F. S. Faria

FEUP, UPorto

Porto, Portugal

up202202471@edu.fe.up.pt

Mohammad S. Javadi

INESC TEC,

Porto, Portugal

msjavadi@gmail.com

Gerardo J. Osório

C-MAST, UBI

Covilha, Portugal

g_osorio@ubi.pt

João P. S. Catalão

SYSTEC-ARISE,

FEUP, UPorto

Porto, Portugal

catalao@fe.up.pt

Abstract—The increase in energy demand and the goal of increasing the share of renewable energies in the energy mix, mostly from intermittent sources, raises concerns about energy storage capacity and the short-medium-term load mismatch of electrical systems. This work proposes an optimal optimization model for the location and capacity of electrical energy storage devices to be installed in a medium or low-voltage distribution network (DN), aiming to reduce the mismatch load between demand and supply of intermittent renewable energy. It considers energy demand response programs using the time-of-use (ToU) program as an incentive to change consumption behavior at times of peak demand on the electricity system. A mixed integer linear programming (MILP) algorithm with multi-criteria decision-making techniques is used to solve the problem, providing some indicators for different investment scenarios. In addition, the model is tested on the IEEE 33-bus test system, where distributed generation sources connected to the medium-voltage (MV) grid are considered. The energy demand varies over a day according to the variation in energy prices in the demand response program.

Index Terms—Demand response program; Electrical energy storage systems; Load mismatch; Smart grid planning.

I. INTRODUCTION

A. Framework and Motivation

Smart grid (SG) is a model that covers the modernization of transmission and DNs, with the fundamental principle of implementing a “digital upgrade” to optimize operations by reducing losses, as well as creating opportunities to create new markets for alternative energy production [1]. This level of high digitalization empowers the SG to have real-time measurements and predictions of electrical variables along the grid that can be used to optimally schedule battery energy storage systems (BESS) [2].

Implementing this transition is important to improve the robustness and regeneration capacity of the network in the event of faults. In SG it is good practice for players to generate and distribute electricity most sustainably. In the European Union (EU), there are some measures to limit the greenhouse gas (GHG) emissions that each company can emit through emission licenses.

If a company has not used up its entire GHG emissions license, it can sell the remaining titles to the European Union Emissions Trading System (EU ETS), other entities may buy and emit more than they are licensed without any legal infringements.

With the previous strategy, since 2005 the EU has managed to reduce GHG emissions from energy-generating units and industry by 37 % [3]. Typically, distributed generation (DG) units are placed in areas of high load density or at the end of network feeders in radial DNs [4], maintaining the electricity system typology hierarchical helping:

- To decrease the power losses because distributed generation is close to loads, reducing fossil fuel consumption in the case of green SG.
- To reduce the investments needed to expand the transmission network, microgrids are the answer to improve the recovery capacity of the DN [5].
- To improve power quality using inverter-based SG, improving the voltage profile and voltage drops, hence, improving power system reliability.

In DGs, electricity can be stored in a variety of ways, mechanically, electrically, or electrochemically. With the increasing integration of renewable energy sources (RES) into the DN, the installation of BESSs in the DN leads to the possibility of mitigating the intermittency through peak shaving, i.e., energy is stored in the BESSs during off-peak periods and the BESSs are discharged during the periods of high energy demand [6].

In SGs, one of the biggest challenges is managing load mismatch. In conventional grids, this problem is managed centrally by the grid operator, creating various challenges such as the great complexity of centrally resolving power traffic, making it difficult to scale the system. On conventional networks, as energy demand increases, the issue of load mismatching is becoming increasingly relevant [7]. The literature shows that with the increased penetration of RES and the uncontrollable characteristics of the grid, there can be a mismatch between intermittent production and consumption, i.e., a residual demand [8].

G.J. Osório acknowledges the support by FCT through UIDB/00151/2020 (<https://doi.org/10.54499/UIDB/00151/2020>) and UIDP/00151/2020 (<https://doi.org/10.54499/UIDP/00151/2020>), C-MAST. M.S. Javadi acknowledges FCT for the funding provided through 2021.01052.CEECIND. J.P.S. Catalão acknowledges the support by the EU Horizon Europe Programme under GA ID: 101160614 (EU-DREAM Project, DOI: 10.3030/101160614).

In [7] proposed an energy management system to be implemented in SG to increase the system's efficiency, based on DN management to allocate the production to loads nearby in the DN, reducing system losses. The research also evaluated the system's resilience in the event of a communication failure between the nodes of the test system.

Hence, with electricity consumption and energy demand growth worldwide [4], demand response programs (DRPs) are a fundamental solution to help make the energy transition. According to some authors, DRP is one of the most practical ways of reducing load mismatch, i.e. the difference between electricity production and consumption [9], [10]. Implementing DRP in the electricity system has several advantages, such as balancing generation and consumption, increasing flexibility, increasing grid reliability and reducing CO₂ emissions [10]. In practice, DRPs allow energy demand to be adjusted to meet the power generation, as opposed to the system operator adjusting the power generation to meet the demand reducing costs [9].

B. Related Work

In [11] a computationally efficient algorithm was proposed for optimizing the location and size of BESSs in a transmission IEEE 24-bus test system considering a ToU DRP. The approach was to divide the problem into two parts, the master problem and the slave problem. The master problem consists of the optimal location and size of the BESS, while the slave problem consists of optimizing the operational point of the generation units and the BESS, using a standard MILP model. At the master level, Binary Particle Swarm Optimization (BPSO) and the Binary Genetic Algorithm (BGA) were used to propose various investment options at the planning level. The slave problem has a short time horizon, optimized for the next day, determining the optimal time for a DG considering the presence of a BESS.

Long-term planning considering the influence of BESSs and DRPs was considered in the work carried out in [12]. The optimization problem was divided in the same way into a master problem and a slave problem. The master level deals with long-term planning, while at the slave level, the optimized operation of the system for the short term is obtained. The DRP implemented the ToU mechanism, tested on a standard 6-Bus, demonstrating a reduction in overall system losses as well as an improvement in the system load factor.

In [13] proposed DGs and BESSs planning for an active DN using bi-level programming. At the master level, DG, and BESSs' location and size are optimized. The slave level focuses on BESSs optimization. The approach used improved binary PSO (IBPSO) and bi-level programming by swapping interactions between the two levels. The results were the reduced planning deviations created by DG's power output. Improvements were in terms of the voltage profile and operational economy in the DN. These results were obtained by simulating the PG&E 69-bus DN.

In [14], a method for allocating a BESS was proposed. The goal was to minimize the daily losses of the DN – accounting for the injection of RES into the network – by optimizing the location and size of the BESS. To solve this model, the authors have developed a modified annealing genetic method with a double-threshold mutation probability control that allows them to avoid trapping the algorithm in a local optimum.

C. Goals and Contributions

Distributed renewable generation does not just create problems for the existing electricity grid, it also helps to solve other important issues, such as reducing power losses and delaying investment in expanding the transmission network by having generation closer to the consumer units. When SG is implemented in the DN, combined with solutions that integrate BESSs, it has enormous potential to relieve the pressure that the automotive electrification growth is bringing [15], growing by 130% between 2021 and 2022 [16], while at the same time opposing the intermittency of DG units, providing an extra source of energy for charging electric vehicles [17].

DNs typically have a radial typology [18] – mainly in rural environments – being more meshed in urban areas. Radial typology brings high challenges in terms of power quality control when there are long feeders. The critical power quality problem is controlling voltage in the regulatory range along feeders, leading to voltage drops at the end of the feeder and overvoltage near substations.

The goal of this work is to present the ideal location and sizing of BESSs in the IEEE 33-Bus DN, to reduce the load mismatch between the production of RES and the system loads, considering the loading and unloading capabilities of BESSs as a DRP. The current work will build on the work previously carried out in [11], adapting it to a DN with its intrinsic characteristics by considering:

- Adaptation of the algorithms to the characteristics of medium-voltage DNs,
- Propose an optimal location for the BESSs in the IEEE 33-Bus model network, as well as the optimal size for each of the BESSs in the IEEE 33-Bus model network,
- Simulate the IEEE 33-Bus model network for various operating zones, analyzing its power flows, power losses, and voltage profiles.

The remaining work is presented as follows: Section II describes the methodology and mathematical formulation. Section III presents the case study data and results analysis. Section IV remarks on the main findings and future guidelines.

II. METHODOLOGY AND MATHEMATICAL INFORMATION

A. Methodology

In this work, the slave problem is carried out repeatedly assuming, for each case, that a BESS is placed on each of the buses (not simultaneously), i.e., for each of the BESS capacity levels to be analyzed, the slave problem will be executed 33 times. A representative day is to estimate the operating cost, total system cost, and minimum and average voltages for each case of BESS placement. The results of these iterations will be analyzed to choose the best bus to place the BESS of a given capacity.

It will also be possible to submit the optimum results for each capacity to the optimum choice process again, resulting in an analysis of which BESS capacity will be most beneficial for the system according to the chosen optimization criteria. The methodology used in this study incorporates multi-criteria decision-making (MCDM) techniques to address complex decision-making scenarios that involve conflicting goals.

Specifically, the Fuzzy Satisfying Method (FSM) and the Technique for Order Preference by Similarity to Ideal Solution (TOPSIS) were employed to evaluate and rank options, helping with the informed decision-making process. The integration of FSM and TOPSIS creates robust evaluating options in MCDM scenarios. FSM addresses uncertainty and vagueness in preference selections, while TOPSIS provides a systematic approach to ranking alternatives based on their proximity to the ideal solutions. When combined, these methodologies establish a comprehensive and reliable analytical framework for making well-informed decisions.

B. Mathematical Information

To determine the optimum capacity and location for installing BESS in a smart DN, using BESS's charging and discharging capabilities as a DRP, Eq. (1) tries to minimize the investment costs (*INVC*) and the total operating costs (*TOPC*) of BESS during their useful life. Eq. (2) represents the master problem, while Eq. (3) represents the slave problem. In the master problem, the interest rate (*r*) and the lifetime of the BESS (*LT*) are considered to calculate the investment cost:

$$\text{Min}(TC) = \text{Min}(INVC + TOPC) \quad (1)$$

where:

$$INVC = \sum_{s=1}^{N_S} \sum_{i=1}^{N_B} \frac{r(1+r)^{LT}}{(1+r)^{LT}-1} [BESS_{i,s} K_{i,s} Cost_{i,s}] \quad (2)$$

$$TOPC = \sum_{t=1}^{N_T} \sum_{i=1}^{N_B} \sum_{s=1}^{N_S} [P_{s,i,t}^{Dis} \lambda_{i,t}^{Dis} \Delta t - P_{s,i,t}^{Ch} \lambda_{i,t}^{Ch} \Delta t] \quad (3)$$

where N_D, N_T, N_B, N_S are the season *d*, time *t*, bus *i*, and BESS device *s*, respectively, *K* is the BESS installation binary decision variable, *Cost* is related to BESS investment cost, *F* is related with the cost of active power generation *PG*, *SUC*, *SDC* are the startup and shutdown cost, respectively, P^{Dis}, P^{Ch} are the BESS power discharging and charging, respectively, together with their respective electricity market prices λ .

For the master problem side, Eq. (4) represents the total acceptable size or capacity of BESS for a given DN. Eq. (5) represents the value of the total budget for investing in BESS in the DN.

$$\sum_{s=1}^{N_S} \sum_{i=1}^{N_B} BESS_{i,s} K_{i,s} \leq BESS^{max} \quad (4)$$

$$\sum_{s=1}^{N_S} \sum_{i=1}^{N_B} BESS_{i,s} K_{i,s} Cost_{i,s} \leq Budget^{max} \quad (5)$$

where *Budget*^{max} is the available budget for BESS installation in (\$) and *Cost* is the BESS investment cost in (\$/MWh). On a commercial level, BESS has standardized sizes and investment costs per kWh of capacity. The BESS costs also vary according to the BESS type.

The slave problem constraints are related to the day-ahead schedule operation of DN, related to the BESS operation and DN power flow constraints. Eq. (6) describes the BESS dynamic energy behavior, while Eq. (7) describes the maximum and minimum energy limits. The initial and final energy level of the BESS is given by Eq. (8), ensuring that the initial and final stored energy remains the same for the entire period of hours considered.

Eq. (9) shows the BESS restriction to inject or absorb reactive energy from the grid. The acceptable power for hourly BESS charging or discharging is given by Eq. (10) and Eq. (11), respectively [19], [20]. The model considers an hourly time interval, and in each hour, BESS can only operate in a charging or discharging state, described by the binary restriction expressed in Eq. (12).

$$Eng_{s,i,t} = Eng_{s,i,t-1} + P_{s,i,t}^{Ch} \eta_s^{Ch} \Delta t - p_{s,i,t}^{Dis} \Delta t / \eta_s^{Dis} \quad (6)$$

$$Eng_{s,i}^{min} \leq Eng_{s,i,t} \leq Eng_{s,i}^{max} \quad (7)$$

$$Eng_{s,i,t=1} = Eng_{s,i,t=24} \quad (8)$$

$$-0.75(P_{s,i,t}^{Ch} + P_{s,i,t}^{Dis}) \leq Q_{s,i,t}^{BESS} \leq +0.75(P_{s,i,t}^{Ch} + P_{s,i,t}^{Dis}) \quad (9)$$

$$0 \leq p_{s,i,t}^{Ch} \leq p_{s,i,t}^{Ch,max} I_{s,i,t}^{Ch} \quad (10)$$

$$0 \leq p_{s,i,t}^{Dis} \leq p_{s,i,t}^{Dis,max} I_{s,i,t}^{Dis} \quad (11)$$

$$0 \leq I_{s,i,t}^{Ch} + I_{s,i,t}^{Dis} \leq 1 \quad (12)$$

Modelling DistFlow [21] in the DN is given by Eqs. (13)-(21). In brief, Eq. (13) and Eq. (14) show the net active and reactive power injection at each bus, respectively. The active and reactive power flows of the network's branches are represented by Eqs. (16)-(17), whereas the generalized power flow equation is presented in Eq. (15). The node voltage restriction is shown in Eq. (18), and the maximum and minimum allowable power generation for both active and reactive power generation are stated in Eqs. (19)-(20). Hence, Eq. (21) models the power feeders' capacity perceived.

$$PG_i - \sum_{l \in \Omega} P'_l - PD_i = 0 \quad \forall i \in \Omega^b \quad (13)$$

$$QG_i - \sum_{l \in \Omega} Q'_l - QD_i = 0 \quad \forall i \in \Omega^b \quad (14)$$

$$P'_i + jQ'_i = V_i \sum_{j \in \Omega} Y_{ij}^* V_j^* \quad \forall l \in \Omega^l, i \neq j \quad (15)$$

$$P'_l = G_l [V_l^2 - V_l V_j \cos(\delta_l - \delta_j)] + B_l V_l V_j \sin(\delta_l - \delta_j) \quad (16)$$

$$Q'_l = B_l [V_l^2 - V_l V_j \cos(\delta_l - \delta_j)] - G_l V_l V_j \sin(\delta_l - \delta_j) \quad (17)$$

$$V_i^{min} \leq V_i \leq V_i^{max} \quad (18)$$

$$PG_i^{min} \leq PG_i \leq PG_i^{max} \quad (19)$$

$$QG_i^{min} \leq QG_i \leq QG_i^{max} \quad (20)$$

$$\sqrt{(P'_l)^2 + (Q'_l)^2} \leq S_l^{max} \quad (21)$$

where P'_l, Q'_l are the net injected active, and reactive power, respectively, and $G_t = R_l / Z_l^2$; $B_l = X_l / Z_l^2$; $Z_l^2 = R_l^2 + X_l^2$, assuming that there exist Ω^l and Ω^b distribution lines and bus sets, respectively. Line *l* resistance and reactance are represented by the variables R_l and X_l , respectively. Power active and reactive demand at bus *i* is represented by PD_i , and QD_i , respectively.

C. Multi-Criteria Decision Analysis

One of the decision-making methods considered in this work is the TOPSIS method. Matrix (22) represents the results for *n* Bus and 4 decision variables, represented by *m*. The results are then normalized by Eq. (23) and inserted in Eq. (24). The normalized results are weighed using the matrix of weights, considering Eq. (25) and Eq. (26).

$$X = \begin{bmatrix} x_{11} & x_{12} & \cdots & x_{1m} \\ x_{21} & x_{22} & \cdots & x_{2m} \\ \vdots & \vdots & \ddots & \vdots \\ x_{n1} & x_{n2} & \cdots & x_{nm} \end{bmatrix} \quad (22)$$

$$r_{ij} = \frac{x_{ij}}{\sqrt{\sum_{i=1}^n x_{ij}^2}} \quad (23)$$

$$R = \begin{bmatrix} r_{11} & r_{12} & \cdots & r_{1m} \\ r_{21} & r_{22} & \cdots & r_{2m} \\ \vdots & \vdots & \ddots & \vdots \\ r_{n1} & r_{n2} & \cdots & r_{nm} \end{bmatrix} \quad (24)$$

$$v_{ij} = w_j \times r_{ij} \quad (25)$$

$$V = \begin{bmatrix} v_{11} & v_{12} & \cdots & v_{1m} \\ v_{21} & v_{22} & \cdots & v_{2m} \\ \vdots & \vdots & \ddots & \vdots \\ v_{n1} & v_{n2} & \cdots & v_{nm} \end{bmatrix} \quad (26)$$

The Calculation of the positive ideal solution A^+ and the negative ideal solution A^- is drawn using the Eq. (27). The Euclidean distance between A^+ and A^- is calculated in Eq. (28), while the relative distance to the ideal solution is carried out in Eq. (29) and the result is the ordering of the best choice, C_i .

$$\begin{aligned} A^+ &= \{\max(v_{ij})|j \in J_1, \min(v_{ij})|j \in J_2\} \\ A^- &= \{\min(v_{ij})|j \in J_1, \max(v_{ij})|j \in J_2\} \end{aligned} \quad (27)$$

$$S_i^+ = \sqrt{\sum_{j=1}^m (v_{ij} - A_j^+)^2}, S_i^- = \sqrt{\sum_{j=1}^m (v_{ij} - A_j^-)^2} \quad (28)$$

$$C_i = \frac{S_i^-}{S_i^+ + S_i^-}, 0 \leq C_i \leq 1 \quad (29)$$

Another method used to support the decision on the optimum location and size for the medium-voltage network is the FSM. It employs fuzzy membership functions to represent the satisfaction levels of various criteria for the decision-making process. These membership functions show the satisfaction degree from the decision feels toward objective values. For each objective function $f_q(X)$, a fuzzy membership function $\mu_{f_q}(X)$ is constructed considering lower and upper bounds, $f_q^{\min}(X)$ and $f_q^{\max}(X)$, established for each criterion, which represent the desirable values [22], noted Eq. (30):

$$\mu_{f_q}(X) = \begin{cases} 0, & \text{if } f_q(X) \geq f_q^{\max}(X) \\ \frac{f_q^{\max}(X) - f_q(X)}{f_q^{\max}(X) - f_q^{\min}(X)}, & \text{if } f_q^{\min}(X) < f_q(X) < f_q^{\max}(X) \\ 1, & \text{if } f_q(X) \leq f_q^{\min}(X) \end{cases} \quad (30)$$

III. CASE STUDY AND RESULTS

A well-known benchmark model for analyzing and exploring the electrical power DN is the IEEE 33-Bus distribution system, with a total active and reactive load of 3.715 MW and 2.3 MVAR, respectively, the model consists of 33 buses and 32 branches. Fig. 1 shows the diagram of the IEEE 33-bus model which, in this case, bus 1 will have a generating unit, that represents an HV/MV substation to feed the medium-voltage network. The medium-voltage network will have a nominal voltage of 12.66 kV. TABLE I shows the characterization of the various case studies carried out in this work. For the master problem, a data set is used and presented in TABLE II, showing the range of capacities that can be installed.

TABLE III shows the weight values for each objective in the algorithms to be used to solve the master problem. TABLE IV shows the technical limits for operating the BESS, namely the maximum and minimum usable energy range, the initial energy and the maximum charging and discharging power.

The substation that connects the high-voltage network to the medium-voltage network has a 6 MVA transformer. The optimal locations for the placement of BESS obtained with TOPSIS for each of the BESS capabilities are summarized in TABLE V. Finally, by carrying out a TOPSIS analysis, once again, considering the best location for the BESS, considering each of the capacity levels, Fig. 2 is obtained, which represents the order of the best capacity choices.

The optimal conditions of the TOPSIS method and FSM with the addition of photovoltaic (PV) generation in the system were simulated for the 10 PV generation scenarios. The results obtained for each of the optimal choices using the TOPSIS method and FSM with the addition of PV are shown in TABLE VI and TABLE VII, respectively. The optimum case using the FSM method has lower total losses than the analysis using the TOPSIS method, as well as a higher average voltage. However, the minimum voltage of the TOPSIS optimal is higher. TABLE VIII denotes the analysis of the results considering the FSM optimal capacity to install.

It is possible to observe that the total losses were reduced considering the analysis carried out with the FSM optimization, while the minimum voltage obtained better results considering the TOPSIS optimization. Regarding the average voltage, the greatest benefit was found with FSM optimization, given the greater proximity of the BESS to the center of the distribution network branches, contributing to an increase, on average, in voltage regulation along all the system's buses.

With a minimum voltage of 0.9131 pu, Case 1, which had no PV or BESS, had a higher operating cost (\$682.11) and notable power losses (3410.538 kW). The operational cost dropped marginally to \$678.28 and the power losses to 3391.380 kW in Case 2.1, where BESS was included but no PV systems were installed.

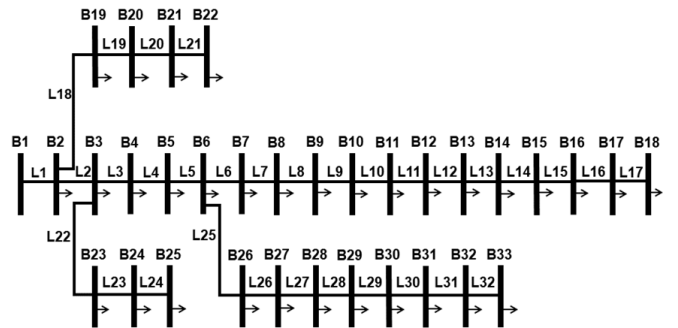


Figure 1. Diagram of the IEEE 33- Bus system.

TABLE I. CASE STUDY TYPES AND THEIR PRESUMPTION

Cases	Algorithm		EESD Allocation	PV Generation
	TOPSIS	FSM		
1	X	X	X	X
2	√	√	√	X
3	X	X	√	√

TABLE II. CANDIDATES LIST FOR PLACEMENT CAPACITY

Possible Capacity of BESS (kWh)			
100	200	250	400

TABLE III. WEIGHT VALUES USED FOR THE TOPSIS AND FSM METHODS

TOPSIS Method				
	Operational Cost	Total Loss	Min Voltage	Average Voltage
Cost Oriented	0.5	0.25	0.15	0.1
Technical Performance	0.1	0.4	0.3	0.2
Reliability Oriented	0.2	0.2	0.4	0.2
FSM Method				
	Operational Cost	Total Loss	Min Voltage	Average Voltage
Reliability Oriented	0.2	0.2	0.4	0.2

TABLE IV. CHARACTERISTICS OF BESS IN OPERATION

$Eng^{BESS,min}$	$Eng^{BESS,max}$	$p^{BESS,Ch,max}$	$p^{BESS,Dis,min}$	$Eng^{BESS,initial}$
20%	100%	20%	20%	50%

TABLE V. SUMMARY OF OPTIMAL BESS LOCATION WITH TOPSIS

BESS (kWh)	BUS	Operational Cost (\$)	Total Loss (kW)	Min Voltage (p.u.)	Average Voltage (p.u.)
100	17	3391.380	3432.946	0.9154	0.956
200	7	3383.376	3474.013	0.9142	0.958
250	7	3376.306	3489.719	0.9145	0.958
400	5	3376.614	3564.268	0.9138	0.958

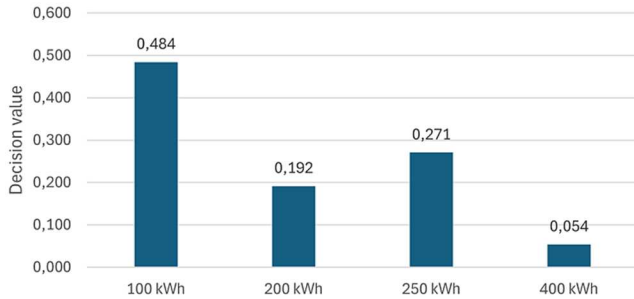


Figure 2. The best-ordered capacity choices with TOPSIS analysis for the BESS capacities.

TABLE VI. OPTIMAL CHOICES USING TOPSIS METHOD WITH PV

Scenario	Operational Cost (\$)	Total Losses (kW)	Minimum Voltage (pu)	Average Voltage (pu)
S1	678.14	3390.71	0.91540	0.95799
S2	678.02	3390.11	0.91540	0.95800
S3	678.18	3390.91	0.91540	0.95798
S4	678.14	3390.68	0.91540	0.95799
S5	678.14	3390.69	0.91541	0.95799
S6	677.98	3389.92	0.91540	0.95800
S7	677.95	3389.75	0.91540	0.95800
S8	678.10	3390.51	0.91540	0.95799
S9	678.16	3390.79	0.91540	0.95799
S10	678.13	3390.67	0.91540	0.95799
Average	678.09	3390.47	0.92	0.96

TABLE VII. OPTIMAL CHOICES USING FSM METHOD WITH PV

Scenario	Operational Cost (\$)	Total Losses (kW)	Minimum Voltage (pu)	Average Voltage (pu)
S1	672.13	3360.64	0.9138	0.9580
S2	671.96	3359.81	0.9138	0.9581
S3	671.99	3359.94	0.9137	0.9580
S4	672.12	3360.60	0.9138	0.9580
S5	671.94	3359.72	0.9138	0.9581
S6	672.10	3360.51	0.9138	0.9580
S7	671.89	3359.45	0.9138	0.9581
S8	671.91	3359.54	0.9138	0.9581
S9	671.96	3359.82	0.9137	0.9581
S10	671.94	3359.70	0.9138	0.9581
Average	671.99	3359.97	0.91	0.96

TABLE VIII. SUMMARY OF OPTIMAL BESS LOCATION WITH FSM

	Oper. Cost	Total Loss	Minimum Voltage	Average Voltage	Decision (kWh)
Cost Oriented	0.5	0.25	0.15	0.1	100/400
Technical Performance	0.1	0.4	0.30	0.2	200
Reliability Oriented	0.1	0.2	0.40	0.2	200

Compared to Case 2.1, Case 3.1 operational costs increased somewhat to \$ 677.95 due to the inclusion of both BESS and PV systems; nevertheless, power losses were still decreased to 3389.752 kW. With a minimum voltage of 0.9154 p.u. and an average voltage of 0.9580 p.u., voltage profiles significantly improved, demonstrating the extra advantages of combining PV systems with BESS for grid stability. Lastly, the best overall performance was demonstrated in Case 3.2, where the FSM approach was used to optimize the location of both BESS and PV systems. The overall losses dropped to 3359.453 kW, the operational cost dropped to \$ 671.89, and the voltage profiles improved even more, reaching an average of 0.95805 p.u. and a minimum of 0.9138 p.u. This case demonstrated how BESS and PV systems work together to create a more reliable, affordable, and resilient grid.

IV. CONCLUSION

The current study assessed the impact of adding BESS on lowering power losses, boosting overall energy efficiency, and optimizing voltage profiles using simulations across several case studies. A multi-objective optimization problem was solved using heuristic techniques, TOPSIS and FSM methods. The capacity of BESS to regulate charging and discharging times allowed for the explicit consideration of DRP integration in this study. The study showed that by employing BESS in this way, BESS may be used to optimize energy consumption patterns and shift peak loads, both of which enhance system performance. The proposed strategy emphasizes how BESS helps with load balancing and cost reduction, which makes it an essential component of further demand-side management research. The case study results show how integrating PV and BESS into medium-voltage DN might be beneficial. Optimizing these systems decreases operating costs, improves voltage stability, and minimizes power losses, especially when paired with cutting-edge techniques like TOPSIS and FSM.

REFERENCES

- [1] T. Vijayapriya and D. Kothari, "Smart Grid: An Overview," *Smart Grid Renew. Energy*, vol. 2, no. 4, pp. 305-311, 2011.
- [2] J. E. R. Baptista, A. B. Rodrigues, and M.G. Silva, "Voltage Profile Assessment in Smart Distribution Grids Considering BESS and Communication Network Failures," *Elect. Power Syst. Res.*, vol. 213, pp. 108660, Dec. 2022.
- [3] What is the EU ETS? - European Commission. Online: https://climate.ec.europa.eu/eu-action/eu-emissions-trading-system-eu-ets/what-eu-ets_en. [Accessed on 20/07/2024].
- [4] S. E. Razavi, *et al.*, "Impact of Distributed Generation on Protection and Voltage Regulation of Distribution Systems: A Review," *Renew. Sustain. Energy Rev.*, vol. 105, pp. 157-167, May 2019.
- [5] J. M. Home-Ortiz, *et al.*, "A Strategy to Enhance the Distribution Systems Recoverability Via the Simultaneous Coordination of Planning Actions and Operational Resources," *Intern. J. Elect. Power Energy Syst.*, vol. 147, pp.108863, May 2023.
- [6] Y. S. Wong, *et al.*, "Stationary and Mobile Battery Energy Storage Systems for Smart Grids," in Proc. *4th Int. Conf. Electric Utility Deregulation and Restructuring and Power Technologies (DRPT)*, Weihai, China, 2011, pp. 1-6, doi: 10.1109/DRPT.2011.5993853.
- [7] N. S. Wade, *et al.*, "Evaluating the Benefits of an Electrical Energy Storage System in a Future Smart Grid," *Energy Pol.*, vol. 38, no. 11, pp. 7180–7188, Nov. 2011.
- [8] T. Lu, *et al.*, "India's Potential for Integrating Solar and On- and Offshore Wind Power into Its Energy System," *Nature Commun.*, vol. 11, no. 1, pp. 4750, Sep 2020.
- [9] M. Vahid-Ghavidel, *et al.*, "Demand Response Programs in Multi-Energy Systems: A Review," *Energies*, vol. 13, no. 17, 2020.
- [10] M. Vahid-Ghavidel, *et al.*, "Energy Storage System Impact on the Operation of a Demand Response Aggregator," *J. Energy Storage*, vol. 64, pp. 107222, Aug. 2023.
- [11] M. S. Javadi, *et al.*, "A Two-Stage Joint Operation and Planning Model for Sizing and Siting of Electrical Energy Storage Devices Considering Demand Response Programs. International," *J. Elect. Power Energy Syst.*, vol. 138, pp. 107912, Jun. 2022.
- [12] M. S. Javadi, *et al.*, "Optimal Sizing and Siting of Electrical Energy Storage Devices for Smart Grids Considering Time-of-Use Programs," in Proc. *45th Annual Conf. IEEE Industrial Electronics Society (IECON 2019)*, Lisbon, Portugal, 2019, pp. 4157-4162, doi: 10.1109/IECON.2019.8927263.
- [13] Y. Li, *et al.*, "Joint Planning of Distributed Generations and Energy Storage in Active Distribution Networks: A Bi-Level Programming Approach," *Energy*, vol. 245, pp. 123226, 2022.
- [14] S. Peng, *et al.*, "Method of Site Selection and Capacity Setting for Battery Energy Storage System in Distribution Networks with Renewable Energy Sources," *Energies*, vol. 19, no. 9, pp. 3899, 2023.
- [15] M. S. Javadi, *et al.*, "Optimal Self-Scheduling of Home Energy Management System in the Presence of Photovoltaic Power Generation and Batteries," *Energy*, vol. 210 pp. 118568, Nov. 2020.
- [16] Portuguese Energy Balance (2023), (Portuguese version). Online: <https://www.dgeg.gov.pt/media/vt3bqpmn/dgeg-ben-2022.pdf>. [Accessed on 26/06/2024]
- [17] M. Esmaeeli, and S. Golshannavaz, "Optimal Allocation of Cloud Energy Storage System in Low-Voltage Distribution Network," *Sustain. Energy Grids Net.*, vol. 34, pp. 101053, Jun. 2023.
- [18] C. Zhu, *et al.*, "Feasibility Analysis of PV and Energy Storage System Integration for Flexible Distribution Networks: A Moment-Based Distributionally Robust Approach," *Energy Reports*, vol. 9, no. 3, pp. 89-98, May 2023.
- [19] M. S. Javadi, A. Anvari-Moghaddam, and J. M. Guerrero, "Robust Energy Hub Management Using Information Gap Decision Theory," in Proc. *43rd Annual Conf. IEEE Industrial Electronics Society (IECON 2017)*, Beijing, China, 2017, pp. 410-415, doi: 10.1109/IECON.2017.8216073.
- [20] S. A. Mansouri, *et al.*, "Stochastic Planning and Operation of Energy Hubs Considering Demand Response Programs Using Benders Decomposition Approach," *Int. J. Elect. Power Energy Syst.*, vol. 120, pp. 106030, Sept. 2020.
- [21] M. S. Javadi, *et al.*, "Optimal Power Flow Solution for Distribution Networks using Quadratically Constrained Programming and McCormick Relaxation Technique," in Proc. *IEEE Int. Conf. Environment and Electrical Engineering (EEEIC2021)*, Bari, Italy, 2021, pp. 1-6, doi: 10.1109/EEEIC/ICPSEurope51590.2021.9584627.
- [22] M. Basu, "An Interactive Fuzzy Satisfying Method Based on Evolutionary Programming Technique for Multiobjective Short-Term Hydrothermal Scheduling," *Elect. Power Syst. Res.*, vol. 69, no. 2, pp.277–285, 2004.